Structural Chemistry (2021) 32:1907–1923
https://doi.org/10.1007/s11224-021-01763-5

ORIGINAL RESEARCH

Investigation of antioxidant activity of epigallocatechin gallate and epicatechin as compared to resveratrol and ascorbic acid: experimental and theoretical insights

Yamina Boulmokh[1] · Karima Belguidoum[1] · Faiza Meddour[2] · Habiba Amira-Guebailia[1]

Received: 24 November 2020 / Accepted: 4 March 2021 / Published online: 31 March 2021

Abstract
Antioxidants are molecules that help the human body to fight oxidative stress caused by excess free radicals that trigger a number of diseases. Understanding the structure–activity relationship of antioxidants and their mechanisms of action is important for designing more powerful antioxidants. Polyphenols from *Vitis vinifera* L. have shown several biological activities among which antioxidant activity. Among polyphenolic compounds having potent biological activities, we find resveratrol (RSV) which is a stilbene and epigallocatechin gallate (EGCg) and epicatechin (EC) which are catechins or flavanols. We report here a comparative study of the antioxidant potential of EGCg and EC as compared to RSV. The most favorable mechanism by which each molecule exerts the antioxidant activity is determined. Ascorbic acid (AA) was included as a reference. DPPH and FRAP assays were used for experimental evaluation of antioxidant activity and for theoretical calculations, density functional theory (DFT) method was chosen. Three mechanisms were investigated: hydrogen atom transfer (HAT), single electron transfer-proton transfer (SET-PT), and sequential proton loss electron transfer (SPLET). Calculated thermodynamic parameters correlate well with percentage inhibition (I%) and half maximal inhibitory concentration (IC50) values given by the DPPH test. Both experimental and theoretical approaches showed that EGCg is more potent antioxidant than EC and RSV. The most preferential sites are gallate moiety and 4′-OH in EGCg and OH sites of the B ring in EC. The pKa values confirm this finding. All proposed mechanisms are favored for EGCg, and SET-PT is preferred antioxidant mechanism for EC and it is the most suitable in the first step for RSV. Flavanols are more potent antioxidants than the stilbene, RSV.

Keywords Catechins · RSV · Antioxidant activity · HAT · SET-PT · DPPH

Introduction

Antioxidant activity is a process in which the antioxidant molecule fights against excess free radicals in the human body. An excess of free radicals leads to oxidative stress that causes alteration of proteins, lipids, and DNA, resulting in the development of various human diseases.

Polyphenols comprising flavonoids such as catechins and stilbenes such as resveratrol (RSV) are secondary metabolites found mainly in plants and fruits. They are powerful antioxidants and their ability to show effective protective effects against oxidative stress is essential for their potential use in therapeutic applications. Among polyphenols of the grapevine *Vitis vinifera* L., we find catechins such as (-)-epicatechin (EC), (-)-epigallocatechin (EGC), (-)-epicatechin gallate (ECG), and (-)-epigallocatechin gallate (EGCg) and stilbenes. Structurally, catechins consist basically of two phenolic rings and an oxygenated heterocycle. Stilbenes are formed by two aromatic rings related by an ethylene bridge. Both stilbenes and catechins contain hydroxyls in their structures. The most striking molecule in the stilbenes family is resveratrol which is the most studied molecule in terms of biological activities and therapeutic use. Catechins and resveratrol have been reported

✉ Yamina Boulmokh
boulmokh.yamina@univ-guelma.dz; m_boulmokh@yahoo.fr

[1] Laboratoire de Chimie Appliquée, Université 8 Mai 1945, BP 401, 24000 Guelma, Algeria

[2] Laboratoire de Chimie Computationnelle et Nanostructure, Université 8 Mai 1945, BP 401, 24000 Guelma, Algeria

to possess a variety of biological and pharmacological properties such as antibacterial potential [1, 2], antimicrobial [3, 4], antioxidant [5–7], and anticancer [8, 9]. They have also been reported to play a role in pandemic diseases [10], in the prevention of age-related cognitive decline [11] and in brain function [12].

Hence, both of these phenolic subclasses have potent antioxidant activity, but we have no idea about which of them is the most powerful antioxidant.

The structure of polyphenolic compounds is linked to their capacity of scavenging the radicals and chelating the metals. It was reported that antioxidant activity of polyphenols or polyhydroxy-phenols is mainly related to the presence of hydroxyl groups [13, 14]. It has also been shown that the more the compound contains OH groups, the higher the antioxidant activity [15–17]. But it was also reported that even if molecules have the same number and position of OH groups, antioxidant activity is different and this is due to other structural features which influence the antioxidant activity [18].

Experimental methods can show that a compound exhibits or not antioxidant activity and enable us to compare the antioxidative potential of a set of molecules, but are unable to show which part or site in molecules are responsible for the antioxidant action. Therefore, it is necessary to perform theoretical studies linking the experimental antioxidant capacity to the structure and the physicochemical properties of compounds having antioxidant activity [19]. The most important feature of computational methods such as density functional theory (DFT), as applied to antioxidant activity studies, is to show which of the sites of molecules is more responsible for antioxidant activity and the reaction mechanisms by which antioxidants can exert their activity.

DFT is a quantum mechanical technique which can be applied for deep understanding of the mechanisms of antioxidant activity of molecules [20–23]. This method allows the calculation of five thermodynamic parameters: bond dissociation enthalpy (BDE), adiabatic ionization potential (AIP), proton dissociation enthalpy (PDE), proton affinity (PA), and electron transfer enthalpy (ETE), which are involved in three main antioxidant mechanisms:

(i) Hydrogen atom transfer (HAT): which is a one-step mechanism in which a hydrogen atom is transferred from the antioxidative molecule to the oxidative radical.

$$ArO{-}H + R^{\cdot} \rightarrow ArO^{\cdot} + R{-}H \quad (1)$$

(ii) Single electron transfer-proton transfer (SET-PT): this mechanism involves two steps. In the first step, a single electron is transferred to free radical and a cation is formed. In the second step, the proton is transferred to the anionic radical.

$$ArO{-}H + R^{\cdot} \rightarrow ArOH^{+\cdot} + R^{-} \quad (2)$$

$$ArOH^{+\cdot} + R^{-} \rightarrow ArO^{\cdot} + R{-}H \quad (3)$$

(iii) Sequential proton loss electron transfer (SPLET): three steps are required in this mechanism. In the first step, a proton is lost and a phenoxide anion is formed. In the second step, an electron is transferred from the phenoxide anion formed to the radical. In the last step, the anionic radical and the proton were combined to produce the new molecule.

$$ArO{-}H \rightarrow ArO^{-} + H^{+} \quad (4)$$

$$ArO^{-} + R^{\cdot} \rightarrow ArO^{\cdot} + R^{-} \quad (5)$$

$$R^{-} + H^{+} \rightarrow RH \quad (6)$$

Highest occupied molecular orbital (HOMO) and lowest unoccupied molecular orbital (LUMO) energies can be associated with the antioxidant activity of molecules [24]. The spin density is an important parameter characterizing the stability of free radicals, because the energy of a free radical can be efficiently decreased if the unpaired electron is highly delocalized through the conjugated system [25]. The enthalpy of acidity and pKa are parameters strengthening the study of the antioxidant activity of the studied compounds. Molecular electrostatic potential (MEP) mapping through a computer-aided method is a very useful approach to explore the reactivity of compounds [26].

The aim of this work is to study the antioxidant activity of three polyphenols; two of them are among the most antioxidants of green tea, these are catechins; EGCg and EC and a stilbene; RSV, an antioxidant found in the grapevine. The study aims at comparing the antioxidant potential of these molecules and showing, by exploiting the three well-known antioxidant mechanisms, which of the sites in each molecule, is more responsible for antioxidant activity. Ascorbic acid (AA) is used here as a standard, for which all parameters were also computed.

This study was achieved by a theoretical DFT method using Gaussian 09. Calculated parameters in the gas phase are BDE, AIP, PDE, PA, ETE, $\Delta H_{acidity}$, pKa, and HOMO and LUMO energies. On the other hand, calculation of the first five parameters was performed in presence of water to show how it would influence as solvent, the individual reaction enthalpies. Besides, spin density contours and electrostatic potential maps were plotted. An experimental procedure was also achieved to compare antioxidant activity of EGCg

and EC to RSV, and AA as a renowned potent antioxidant is used here as a reference. Experimental antioxidant activity was evaluated on the basis of inhibition of the 2,2-diphenyl-1-picrylhydrazyl (DPPH) free radical and ferric reducing power (FRAP) which consists in reducing the colorless Fe^{3+} ion of tripyridyltriazine Fe (TPTZ)$^{3+}$complex into intense blue Fe^{2+} ion, upon reaction with antioxidants. Percentage inhibition of DPPH (I%), IC50, and the reducing power of the studied molecules was evaluated. An attempt was made to correlate experimental results to computational ones.

Methods

Experimental method

Reagents and apparatus

All reagents ((-)-epicatechin, (-)-epigallocatechin gallate, trans-resveratrol, ascorbic acid, DPPH (2,2-diphenyl-1-picrylhydrazyl), trichloroacetic acid, ferric chloride and potassium phosphate) were purchased from Sigma-Aldrich (Germany). For reading absorbance, a UV-visible spectrophotometer (DR6000 HACH, France) was used.

Antioxidant activity procedures

DPPH radical scavenging method

The experimental protocol used is based on conditions previously used by Bougandoura and Bendimerad [27] with small modifications. The DPPH solution is prepared by solubilizing 2 mg of this product in 100 ml of methanol. A volume of 1.95 ml of this solution is added to 50 µl of each of the methanolic solutions of EGCg, EC, RSV, and AA at various concentrations (0.05 to 1 mg/ml). In parallel, a negative control is prepared by mixing 50 µl of methanol with 1.95 ml of methanolic solution of DPPH. After 30 min of incubation in the dark and at room temperature, the absorbance is read at 517 nm. For each concentration of the four molecules' solutions, the assay is carried out in triplicate. The results were expressed as percent inhibition (I%).

$$I\% = [(Abs_{control} - Abs_{test})/Abs_{control}] \times 100.$$

where

Abs_{test} absorbance of the samples.
$Abs_{control}$ absorbance of the negative control.

FRAP method

The experimental protocol used is based on conditions previously optimized by Ferreira et al. [28] with small modifications. One milliliter of each methanolic solution of EGCg, EC, RSV, and AA at different concentrations (from 0.005 to 1 mg/ml) is mixed with 2.5 ml of a 0.2 M sodium phosphate buffer (pH 6.6) and 2.5 ml of 1% potassium ferricyanide $K_3Fe(CN)_6$. The mixture is incubated at 50 °C for 20 min. After that, 2.5 ml of 10% trichloroacetic acid are added to stop the reaction and the mixture was centrifuged at 4000 rpm for 10 min. The upper layer (2.5 ml) is combined with 2.5 ml of distilled water and 0.5 ml of solution of $FeCl_3$ 0.1% (ferric chloride) freshly prepared. The absorbance of the reaction medium was read at 700 nm. An increase in absorbance corresponds to an increase in the reducing power of tested compounds.

Theoretical method details

In this study, optimization energies of different neutral molecules (Fig. 1), radicals, cations, and anions were carried out by DFT method with 6-311++G(d,p) basis set and B3LYP functional, with the aim of calculating BDE, AIP, PDE, PA, ETE, $\Delta H_{acidity}$, and pKa as thermodynamic parameters. The B3LYP is known to provide accurate results of structure and thermodynamic properties of phenolic compounds [29].

The feasibility of different mechanisms is studied by the calculation of five parameters using the following equations:

$$\text{For HAT}: \mathrm{BDE} = H(\mathrm{ArO}^{\cdot}) + H(\mathrm{H}^{\cdot}) - H(\mathrm{ArOH}) \quad (7)$$

$$\text{For SET-PT}: \mathrm{AIP} = H(\mathrm{ArOH}^{+\cdot}) + H(e^{-}) - H(\mathrm{ArOH}) \quad (8)$$

$$\mathrm{PDE} = H(\mathrm{ArO}^{\cdot}) + H(\mathrm{H}^{+}) - H(\mathrm{ArOH}^{+\cdot}) \quad (9)$$

$$\text{For SPLET}: PA = H(ArO^{-}) + H(H^{+}) - H(ArOH) \quad (10)$$

$$\mathrm{ETE} = H(\mathrm{ArO}^{\cdot}) + H(\mathrm{e}^{-}) - H(\mathrm{ArO}^{-}) \quad (11)$$

HOMO, LUMO, and spin density were calculated using the basis 6-311G(d,p) with and without diffuse function. Spin density was determined using both Hartree Fock (HF) and DFT methods.

To determine polyphenols' acidity, two methods were investigated, the first one is the calculation of pKa and the second one is the determination of the enthalpy difference between the anion (A^{-}) and its neutral species (HA).

pKa was determined by application of the following thermodynamic cycle [30]:

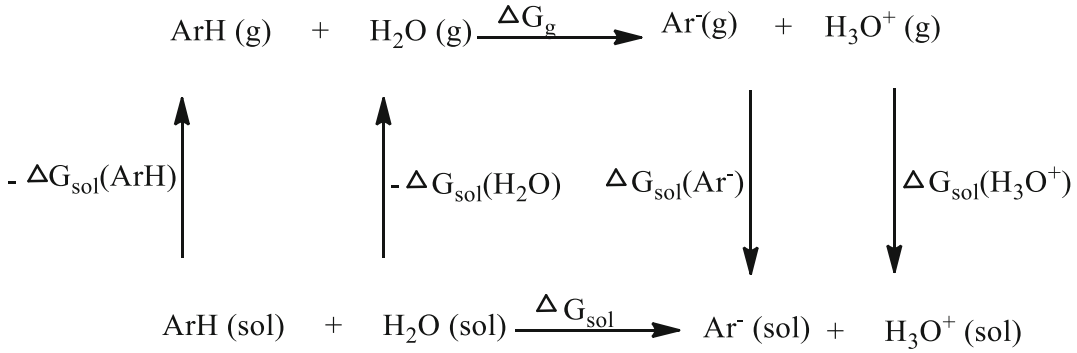

ΔG_{sol} values for H_3O^+ and H_2O were determined experimentally and reported as

−110.2 kcal/mol [30] and −6.31 kcal/mol [31] respectively.

$$\Delta G_{sol} = \Delta G_g + \Delta G_{sol}(Ar^-) + \Delta G_{sol}(H_3O^+) - \Delta G_{sol}(ArH) - \Delta G_{sol}(H_2O) \quad [30] \tag{12}$$

$$pk_a = \frac{\Delta G_{sol}}{1.364} - \log [H_2O] \quad [30]. \tag{13}$$

The concentration of bulk water is 55.49 M [30].

$$pk_a(\text{corrected}) = pk_a(\text{calculated}) - 4.54 [30]. \tag{14}$$

The gas phase acidity is computed at 298 K as the enthalpy difference between the anion (A^-) and its neutral species (HA):

$$\Delta_{\text{Hacidity}} = H(A-) - H(HA) \tag{15}$$

Calculations and structures were performed by Gaussian 09 [32] and Gauss View 5.0.

Results and discussion

Experimental evaluation of antioxidant activity of EGCg, EC, and RSV

Scavenging and inhibition of the DPPH radical

Results of DPPH free radical percentage inhibition for EGCg, EC, RSV, and AA are shown in Fig.2. The free radical percentage inhibition increases with increasing concentration.

According to Fig. 2, for the concentration range of 0.05 to 1 mg/ml, the percentage inhibitions (I%) of the DPPH radical by EGCg, ranging from 28 to 57%, were higher than those of RSV (from 22 to 45%) and AA (5 to 15%). For EC, I% (from 18.7 to 40%) were lower than those of AA but higher than those of RSV.

For concentrations from 0.2 to 1.0 mg/ml, I%, ranging for EGCg from 68 to 86% and for EC from 55 to 81%, were higher than those of RSV (37–46%) but lower than those of AA (90–94%). These results indicate that EGCg is more effective than EC for radical scavenging activity, which agrees with what was reported by He et al. [33]. It is worth noting that some authors such as Guo et al. [34] and Nanjo et al. [35] revealed the importance of the gallate moiety and trihydroxyl group in scavenging the DPPH radical.

Our results also show that EGCg and AA are more susceptible to donate protons to neutralize the DPPH radical.

Determination of IC50

The IC50 is the concentration of the antioxidant required to reduce the original amount of radical by 50% [36]. IC50 value which decreases with increasing antioxidant activity of the samples tested was determined graphically from the corresponding linear regression equation. IC50 values are summarized in Table 1.

According to the results presented above and taking into account IC50 values, AA is the most strong antioxidant (IC50 = 0.026 mg/ml) followed by EGCg (IC50 = 0.047 mg/ml), EC (IC50 = 0.289), and lastly RSV (IC50 = 0.939).

The ferric reduction antioxidant power

Catechins were most reactive and showed the highest stoichiometry of Fe^{3+} in the FRAP assay compared to other flavonoids [37].

The results obtained allowed us to plot the curves representing the variation of the reducing power expressed as the absorbance vs concentration (Fig. 3).

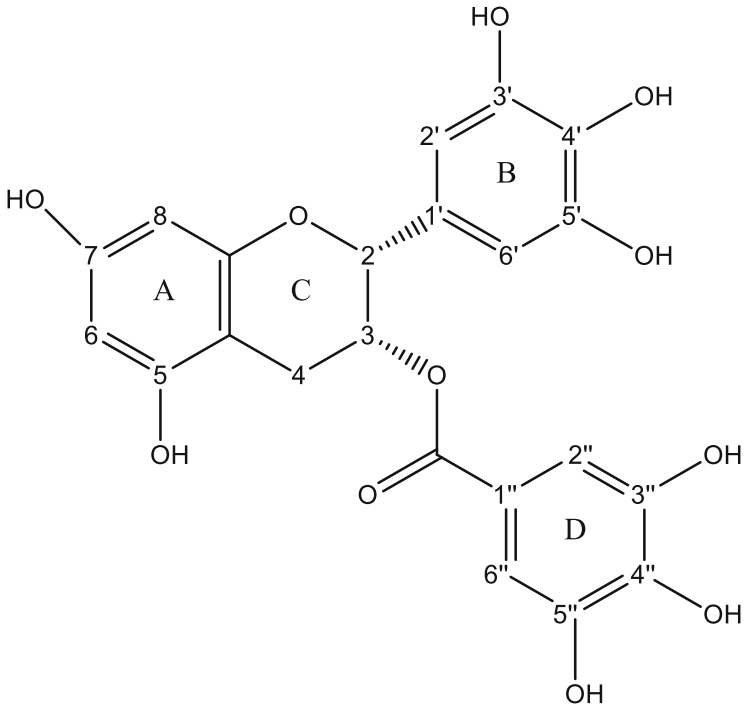

-(-) Epigallocatechin gallate (EGCg)

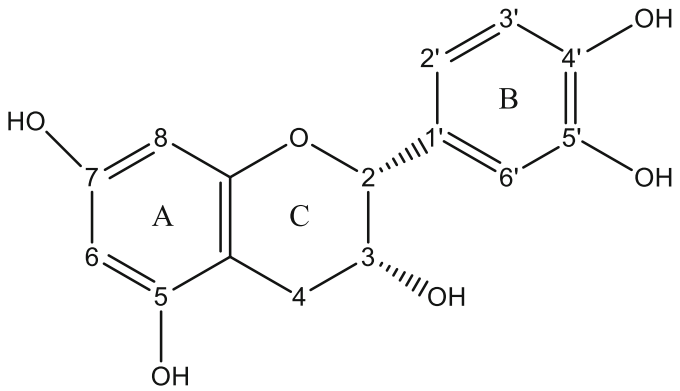

-(-) Epicatechin (EC)

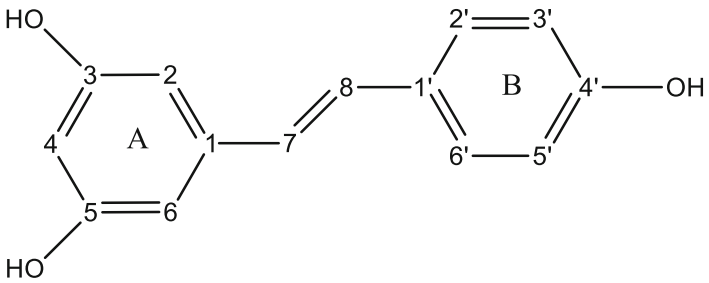

Trans resveratrol (RSV)

Fig. 1 **a** Molecular structure of -(-) epigallocatechin gallate (EGCg), -(-) epicatechin (EC), resveratrol (RSV), and ascorbic acid (AA). **b** B3LYP/6-311++ G(d,p) fully optimized geometries of studied molecules

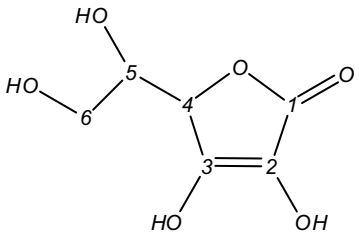

Ascorbic acid (AA)

a

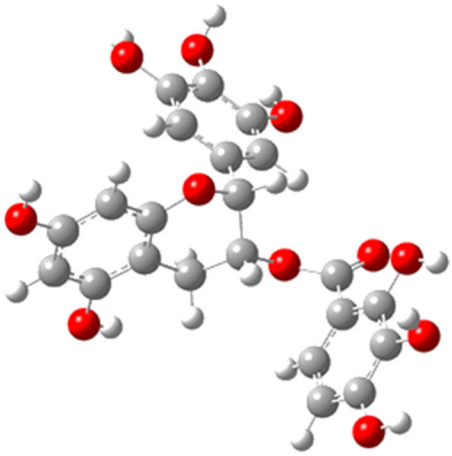

EGCg

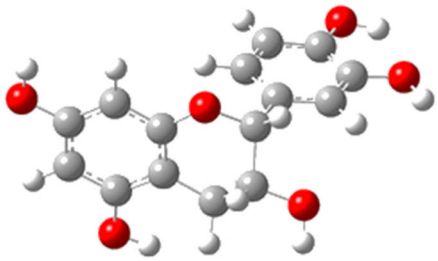

EC

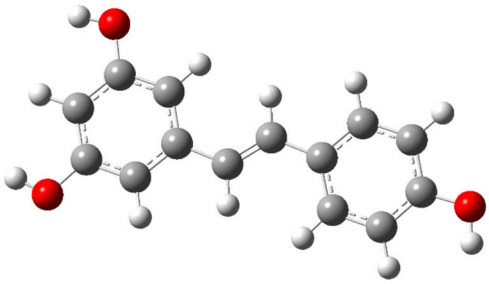

RSV

b

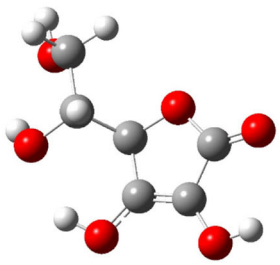

AA

Fig. 1 (continued)

The increase in the absorbance of the reaction medium means an increase in the reduction of iron which increases with increasing concentration of tested molecules.

In view of these results, EGCg has an antioxidant activity greater than that of EC, which is consistent with literature as many authors already reported that catechin gallate esters (EGCg) are more effective for FRAP scavenging than EC [33]. This powerful activity is not only due to the higher number of hydroxyl groups in EGCg but to other features as revealed by theoretical calculations presented below.

For concentrations ranging from 0.005 to 0.2 mg/ml, the reducing power of RSV and the two catechins (Abs = 0.197–1.907 for EGCg and Abs = 0.187–1.786 for EC) is greater than that of AA. Above these concentrations, the reducing capacity of catechins increases but remains lower than that of AA. RSV is the most potent for reducing the ferric cation.

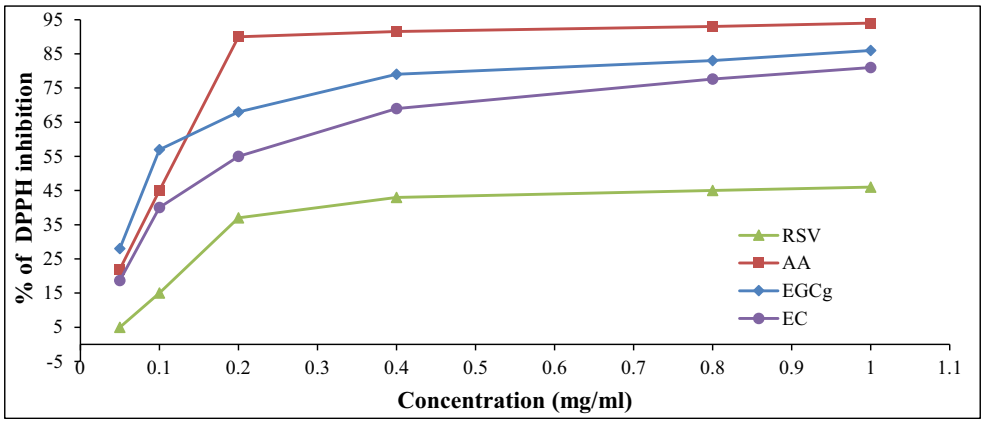

Fig. 2 Percent inhibition of DPPH vs concentration of EGCg, EC, RSV, and AA

Theoretical evaluation of antioxidant activity of EGCg, EC, and RSV

Mechanisms of antioxidant activity

Three mechanisms have been studied in order to determine the most suitable for evaluating the antioxidant activity of EGCg and EC in comparison with RSV as a potential antioxidant and AA included as a reference. Calculations have been performed in the gas phase and in water as selected solvent.

Hydrogen atom transfer

To study HAT mechanism, bond dissociation energies (BDEs) were calculated. BDE is a numerical parameter characterizing the stability of the bond in the hydroxyl group. The weaker this bond, the higher the antioxidant activity, and hence, the more favorable the reaction with free radicals. Therefore, the molecules with low BDE values are expected to show high antioxidant activity. Calculated BDE values for studied compounds are presented in Table 2.

Our results reveal that for EGCg, the lowest value of BDE (300.45 kJ/mol) was observed for 4′–OH, followed by 4″–OH (307.78 kJ/mol) and 5′–OH (331.76 kJ/mol). 5″–OH and 3′–OH sites have almost identical BDE values (337.58 and 337.63 kJ/mol respectively), indicating that these two OH groups are similar in their stability and probability of H– atom donating. These results are in concordance with literature [26].

For EC, the most interesting sites in the B ring are 4′–OH with a BDE value of 336.01 kJ/mol and 5′–OH with a BDE value of 338.41 kJ/mol. These two BDEs are closer to those of 3′–OH and 5″–OH of EGCg but greater than 4′–OH and 4″–OH in EGCg. This is one of the reasons for which EGCg is better antioxidant than EC.

For RSV, the BDE (351.44 kJ/mol) of 4′-OH is the lowest, followed by the 3–OH (369.93 kJ/mol) and finally 5–OH (371.60 kJ/mol). We can notice that all BDE values of RSV are greater than 325 kJ/mol, this result is in agreement with literature [38, 47].

It should be mentioned that five of the eight OHs of EGCg have BDE values less than those of RSV and our results also show that the lowest BDE value of RSV is higher by 51 kJ/mol than that of EGCg, and that is one of the reasons for which EGCg is more potent antioxidant than RSV. For EC, 4′–OH and 5′–OH have BDEs less than all OH BDEs of RSV and this is why EC is better antioxidant than RSV according to the HAT mechanism. BDE values found for OHs in the pentacycle of AA are lower than those outside the pentacycle, this result is in agreement with literature [41]. As can be clearly seen from results in Table 2, BDE values of EGCg in gallate moiety (ring D), EC, and RSV in the B ring are lower than those of AA in pentacycle. On the other hand, BDEs of EGCg, EC and RSV in A and C rings are lower than those of AA outside the pentacycle. AA has been proven experimentally as a potent antioxidant, our results led us to conclude that the HAT mechanism is favored for EGCg, EC, and RSV but not for AA.

Table 1 IC50 values of EGCg, EC, RSV, and AA

Molecule	EGCg	EC	RSV	AA
IC50	0.047	0.289	0.939	0.026

Single electron transfer-proton transfer mechanism

The AIP parameter is related to the SET mechanism. It describes the process of electron donation by the antioxidant. Molecules with low AIP values are more susceptible to ionization and have stronger antioxidant properties. The values of AIP for studied molecules are presented in Table 2. It should be mentioned that a slight difference in AIP values between EGCg and EC (1.6 kJ/mol) is observed; however, the difference in AIP values between RSV and EC is rather higher and equals 35 kJ/mol. Hence, AIP values follow the sequence: RSV< EC ≈ EGCg < AA.

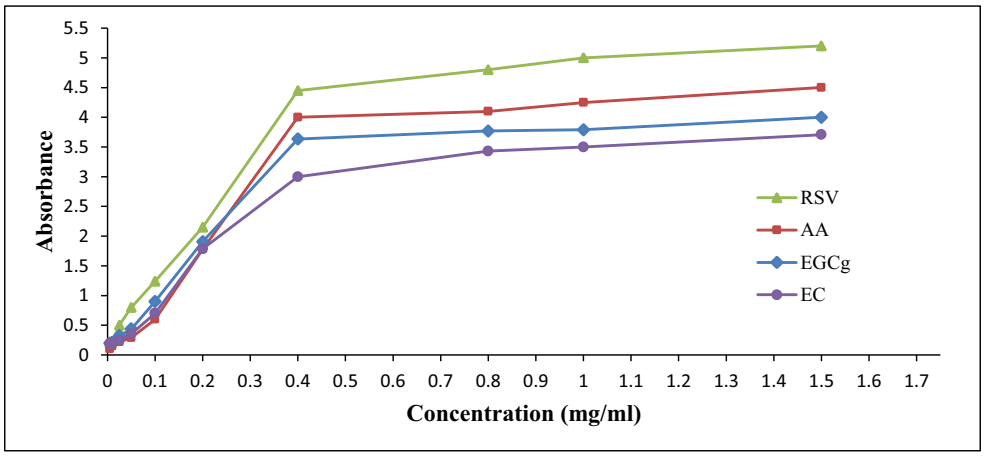

Fig. 3 Reducing power of EGCg, EC, RSV, and AA

To study single electron transfer followed by proton transfer, PDE values were calculated. PDE is an important physical parameter describing the antioxidative properties of the compound investigated as it shows its ability to donate protons. As a rule, compounds with lower PDE values are more susceptible to proton abstraction and hence are the most potent antioxidants.

The calculated PDE values for EGCg, EC, and RSV in the gas phase are presented in Table 2. Our results indicate that lowest PDE values for EGCg are found for OHs in the B ring and in the gallate moiety and 4′–OH is the most acidic. This result reinforces that of HAT transfer and led to conclude that the 4′–OH in the B ring is the most susceptible to H-abstraction. The other values of PDE for EGCg are closer to those of EC and are greater than 950 kJ/mol. These results also corroborate with those of BDE. The PDE values of all OHs of RSV are greater than 1000 kJ/mol and are higher than those of both EGCg and EC OHs, except PDE of 3–OH in EC. As shown in Table 2, the 4′–OH of RSV is more acidic than the other two hydroxyl groups and these results are in agreement with those reported by Fukuhara et al. [48] and Mikulski et al. [44], who claimed that the 4′–OH group of RSV is the most reactive and determines its biological activity. It can be noticed from our results that OH acidity in the pentacycle of AA is comparable to that of 4′–OH in EGCg. On the other hand, PDE values for OH groups outside the pentacycle in AA are comparable to those of OHs in A ring of EGCg and EC. The sequence for PDE is: EGCg ≈ AA < EC < RSV.

It should be inferred from these results, that SET-PT is the most preferred antioxidant mechanism for catechins and the most suitable in the first step for RSV.

Sequential proton loss electron transfer mechanism

The SPLET mechanism is primarily governed by the ease of deprotonation, which can be described by the PA values, and secondarily by the ease of electron transfer from the anions, described by the ETE.

Regarding the deprotonation step, PA values in Table 2 show that EGCg OHs in the gallate moiety are deprotonated considerably easier than the other OH sites and overall, PA values in the gallate lie in a very narrow (1322.19–1358.64 kJ/mol) range. Additionally, with the exception of the gallate moiety, the data of Table 2 confirm that low proton affinities are related to OH groups in the B ring as it was ordinary in most polyphenols such as flavonoids and stilbenes [38, 49, 50]. PA values of hydroxyls in the B ring of EGCg are higher than those of the gallate moiety but lower than those of EC and RSV. The most acidic protons in EC are 4′–OH and 5′–OH, followed by protons of the A ring and lastly by the proton of 3–OH in the C ring. The lowest PA value (1433.49 kJ/mol) for RSV was found for 4′–OH. This result was expected since previous results confirmed the high reactivity of this site.

It is worth noting that the calculated PA values of AA are comparable to those of 4′–OH and hydroxyls of the gallate moiety of EGCg, so EGCg deprotonates as much easily as AA, and hence, EGCg can be qualified as a potent antioxidant.

After deprotonation, the anions may proceed to form the corresponding radicals by electron transfer (measurable by ETE). From the thermodynamic cycle for SPLET, it follows that the larger the PA, the lower the ETE and vice versa.

Our results show that all ETE values for the OH groups in gallate moiety of EGCg are higher than those of the B ring in EGCg and all OHs of EC and RSV. In EC, it was observed that the lowest ETEs were found for anions formed from OH groups located in the B ring. The highest value (424.80 kJ/mol) was found for the 6–OH in AA.

The results of PA and ETE confirm that the SPLET mechanism is more favored for EGCg than EC and RSV.

The effect of water medium on thermodynamic parameters

In view of the results obtained from thermodynamic parameters, calculated in the aqueous phase for the studied molecules, we can stipulate that calculated BDEs in the gas phase and in

Table 2 BDE, AIP, PDE, PA and ETE of EGCg, EC, RSV, and AA in kJ/mol obtained at B3LYP/6-311++ G(d,p) level of theory, in the gas phase

Molecule		BDE	AIP	PDE	PA	ETE	Ring
EGCg	5–OH	375.88	708.88	995.01	1444.48	259.41	A
	7–OH	377.41		996.54	1463.07	242.36	A
	3′–OH	337.63		956.76	1409.52	270.74	B
	4′OH	300.45		919.59	1387.30	241.17	B
	5′–OH	331.76		950.89	1410.37	249.41	B
	3″–OH	333.02		952.15	1337.46	323.57	D
	4″–OH	307.78		926.91	1358.64	277.15	D
	5″–OH	337.58		956.71	1322.19	343.41	D
EC	3–OH	439.59	707.28	1060.32	1494.76	272.85	C
	5–OH	364.98		985.71	1445.44	247.56	A
	7–OH	378.23		998.96	1471.66	234.58	A
	5′–OH	338.41		959.14	1433.73	232.70	B
	4′–OH	336.01		956.74	1430.54	233.48	B
RSV	3–OH	369.93	672.24	1025.70	1457.54	240.40	A
		343.13[a]	658.72[a]	989.82[c]	1443.85[a]	207.32[a]	
		348.2[b]	683.73[e]	1375.12	1423.70[c]	242.02[c]	
		345.26[c]	674.23[f]	1024.93[h]	1473.03[h]	210.63[i]	
	5–OH	371.60	656.51[g]	1027.37	1459.98	239.64	A
		342.13[a]		989.82[c]	1441.55[a]	210.75[a]	
		353.6[b]		1026.02[i]	1423.70[c]	242.02[c]	
		345.26[c]			1474.99[h]	201.60[h]	
	4′–OH	351.44		1007.21	1433.49	245.97	B
		325.49[a]		970.17[c]	1412.29[a]	222.33[a]	
		325.7[b]		1348.39	1396.95[c]	249.12[c]	
		325.62[c]		1006.71[h]	1443.27[h]	222.16[h]	
AA	2–OH	362.75	794.81	895.96	1474.07	216.69	Inside the pentacycle
		324.12[d]	995.6[d]				
	3–OH	357.23		890.43	1370.95	314.29	Inside the pentacycle
		289.46[d]					
	5–OH	463.27		996.48	1370.95	420.34	Outside the pentacycle
		398.75[d]					
	6–OH	452.29		985.50	1355.51	424.80	Outside the pentacycle
		417.86[d]					

[a] [38]
[b] [39]
[c] [40]
[d] [41]
[e] [42]
[f] [43]
[g] [44]
[h] [45]
[i] [46]

water are close to each other for all compounds. The largest deviation between BDE values in the two phases is only 17.77 kJ/mol, which is in concordance with literature [51]. It has been stressed that the gas phase and water BDE values follow the same trend except for 3′–OH and 5″–OH sites in EGCg and for 2–OH and 3–OH for AA; however, in the two environments, the most preferred sites for antioxidant activity are in gallate moiety for EGCg and in B rings for all polyphenolic compounds.

From results presented in Table 3, we can notice that PDE and PA values in water medium, ranging from −34.36 to 110.08 kJ/mol and from 87.48 to 221.57 kJ/mol, respectively, are dramatically lower than those found in the gas phase (890.43–1060.32 kJ/mol for PDE and 1322–1494.76 kJ/mol

Table 3 BDE, AIP, PDE, PA, and ETE in kJ/mol obtained at B3LYP/6-311++ G(d,p) level of theory, in water, for EGCg, EC, RSV, and AA

Molecule		BDE	AIP	PDE	PA	ETE	Ring
EGCg	5–OH	363.27	470.67	17.49	152.53	335.63	A
	7–OH	366.82		21.04	161.85	329.86	A
	3′–OH	338.45		-7.32	131.08	332.26	B
	4′OH	313.89		-31.87	117.00	321.78	B
	5′–OH	334.94		-10.82	131.20	328.64	B
	3″–OH	338.06		-7.71	104.25	358.70	D
	4″–OH	321.22		-24.54	110.92	335.19	D
	5″–OH	342.98		-2.79	87.48	380.38	D
EC	3–OH	447.34	462.15	110.08	221.57	350.66	C
	5–OH	362.69		25.43	157.38	330.19	A
	7–OH	369.19		31.94	169.17	324.91	A
	5′–OH	340.79		3.53	145.83	319.85	B
	4′–OH	338.36		1.10	144.62	318.63	B
RSV	3-OH	368.78	422.05	72.55	164.55	329.12	A
		343.97[a]	519.61[a]	82.63[c]	202.73[d]	333.56[d]	
	5–OH	370.68	497.16[b]	73.52	165.71	329.86	A
		344.93[a]		84.39[c]	202.73[d]	333.56[d]	
	4′–OH	344.12		46.96	156.23	312.78	B
		322.36[a]		59.48[c]	193.11[d]	315.17[d]	
AA	2–OH	344.98	504.24	-34.36	153.18	316.69	Inside the pentacycle
	3–OH	350.51		-28.83	103.52	371.88	Inside the pentacycle
	5–OH	465.17		85.82	103.52	486.54	Outside the pentacycle
	6–OH	455.19		75.84	95.51	484.57	Outside the pentacycle

[a] [38]
[b] [44]
[c] [46]
[d] [40]

for PA), this is due to the high solvation enthalpies of proton [52].

Due to their charge, cationic radicals are sensitive to the polarity of water; as expected, the AIP values in water (422.05–504.24 kJ/mol) are considerably lower than those of the gas phase (672.24–794.81 kJ/mol) for all studied molecules.

According to the SPLET mechanism, electron transfer tendency is studied as the second step by estimating ETEs. It can be seen that the values of this thermodynamic parameter of all compounds are higher in the water medium (312.78 to 486.54 kJ/mol) than the gas phase (216.69 to 424.80 kJ/mol). This is in line with results obtained by many authors such as Anitha et al. [29].

PDE, PA, and AIP values follow the same sequence for both phases while ETE values in the gas phase do not always follow the same trend as in water medium.

We can conclude from the values obtained by the calculation of BDE, PDE, and PA in the aqueous phase that the second step of SET-PT and the first step of SPLET mechanisms are more dominant and preferred than HAT mechanism in all studied molecules.

Frontier orbitals, spin density, and electrostatic potential maps

HOMO and LUMO are among the most important parameters of the molecular electronic structure. According to front orbital theory in DFT [53], the higher the HOMO energy of a molecule, the easier it loses electrons and the faster the reaction of electron donating is. On the other hand, the lower LUMO energy of a molecule indicates its ability to accept electrons.

As shown in Table 4, the use of diffuse function caused a decrease in HOMO and LUMO energies for all molecules. Results indicate that EC is slightly more electron donating than EGCg.

Our results also show that EGCg and RSV have the same LUMO energy (−1.65 eV) in the presence of diffuse function. We should mention that our results for HOMO and LUMO values of RSV are in good concordance with literature [40, 55].

The lowest values of HOMO energy for both basis set were found for AA. When diffuse function was used, HOMO energy for AA decreased slightly from −6.13 to −6.45 eV which is closer to the value reported in the literature (−6.329 eV) [57]. On the other hand, the value of LUMO of AA is greater

Table 4 HOMO and LUMO energies of EGCg, EC, RSV, and AA obtained at B3LYP/6-311G(d,p) level of theory with and without diffuse function

Basis set 6-311++G(d,p)	HOMO (eV)	LUMO (eV)	Gap (eV)
EGCg	−6.10	−1.65	4.45
EC	−5.99	−0.76	5.23
RSV	−5.62	−1.65	3.97
	−5.618[a]	−1.661[a]	3.95[a]
	−5.58[b]	−0.62[b]	4.96[b]
AA	−6.45	−1.07	5.38
Basis set: 6-311G(d,p)	HOMO (eV)	LUMO (eV)	Gap (eV)
EGCg	−5.89	−1.22	4.67
EC	−5.78	−0.22	5.56
RSV	−5.46	−1.44	4.02
	−5.21[c]	−1.15[c]	4.03[c]
	−5.48[d]	−1.45[d]	3.95[d]
	−5.21[e]	−1.17[e]	4.04[e]
AA	−6.13	−0.71	5.42
Basis set : 6-311++G(d,p)	HOMO (eV)	LUMO (eV)	Gap (eV)
EGCg	−6.10	−1.65	4.45
EC	−5.99	−0.76	5.23
RSV	−5.62	−1.65	3.97
	−5.618[a]	−1.661[a]	3.95[a]
	−5.58[b]	−0.62[b]	4.96[b]
AA	−6.45	-1.07	5.38
Basis set: 6-311G(d,p)	HOMO (eV)	LUMO (eV)	Gap (eV)
EGCg	−5.89	−1.22	4.67
EC	−5.78	−0.22	5.56
RSV	−5.46	−1.44	4.02
	−5.21[c]	−1.15[c]	4.03[c]
	−5.48[d]	−1.45[d]	3.95[d]
	−5.21[e]	−1.17[e]	4.04[e]
AA	−6.13	−0.71	5.42

[a] [40]

[b] [42] (B3LYP/6-31+G(d,p))

[c] [54] (B3LYP/6-31G(d))

[d] [55] (B3LYP/6-31G(d,p))

[e] [56] (B3LYP/6-31G(d;p))

than that of EGCg and RSV but lower than that of EC with or without diffuse function.

The high reactivity of compounds is characterized by a small energy gap ($\varepsilon_G = E_{HOMO} - E_{LUMO}$) between the HOMO and the LUMO energies and also by a low LUMO energy, this means that these compounds can behave as soft electrophiles [58, 59]. Reactivity of the studied compounds follows the trend: RSV > EGCg > AA ≈ EC.

The contours of HOMO and LUMO for the neutral species of studied compounds are displayed in Fig. 4.

The π-cloud in the HOMO of EGCg is distributed on the A and C rings, and the π-cloud in the LUMO is distributed on the D ring (gallate moiety). For EC, the π-cloud in the HOMO and LUMO is almost distributed on the three rings. For RSV, it can be noticed that the HOMO and LUMO are distributed on the whole molecule. For AA, The HOMO is concentrated on the pentacycle while the LUMO is distributed on almost the whole molecule.

The antioxidant activity of the compounds can be determined by an interpretation of the spin density values of the radical species studied. Total spin density characterizing the distribution of electron spin in free radicals is responsible for radicals' stability and it is one of the most important quantum properties of radicals. The more delocalized the spin density in the radical, the easier the radical is formed and thus the lower the BDE [60]. In our study, spin density was calculated by HF and DFT, because according to some authors [61–63], DFT overestimates spin density values.

The results of spin density calculated by DFT at B3LYP/6-311G(d,p) including or not diffuse function are almost the same, but they are not in harmony with those calculated by HF method. From results in Table 5, we can see that the values of spin density for radicals formed after H-abstraction obtained by HF/6-31G method are almost half of those obtained by DFT B3LYP/6-311G(d,p).

For EGCg, spin densities allow us to conclude that the 3″–O radical in gallate moiety is the most stable, followed by 3′–O, 5′–O, and 5″–O radicals. The most stable radicals in EC and RSV are 3–O and 4′–O, respectively, according to HF calculations. But according to DFT results, 4′O in EC and 5′–O in EGCg are the most stable. In AA, we recorded the lowest spin density value by HF method but at the same time the highest by DFT attributed to the 6–O radical.

According to results displayed in Table 5 and combining the three mechanisms and spin densities evaluated by DFT, we can conclude that the pharmacophores designated for each molecule are:

- 4′–OH, 5′–OH, and 3”–OH for EGCg
- 5′–OH and 4′–OH for EC
- 4′–OH for RSV
- 3–OH and 2–OH for AA.

If we take a closer look at spin density images, we find that for EGCg, the spin density on 5–O and 7–O radicals is concentrated on the A ring. For 3′–O, 4′–O, and 5′–O radicals, spin density is distributed on the B ring. For 3″–O, 4″–O, and 5″–O radicals, the unpaired electron is located on the gallate moiety.

For EC, the unpaired electron of 3–O position is distributed over the B and C rings. For 5–O and 7–O radicals, the spin density is located on both A and C rings. 5′–O and 4′–O spin densities are located on the B ring only.

On the other hand, in 4′-O radical of RSV, the unpaired electron is disposed on the whole molecule as shown in spin density contours (Fig. 5), while for the 3–O and 5–O radicals, the unpaired electron is mainly located on the A ring and ethylene bridge (Fig. 5).

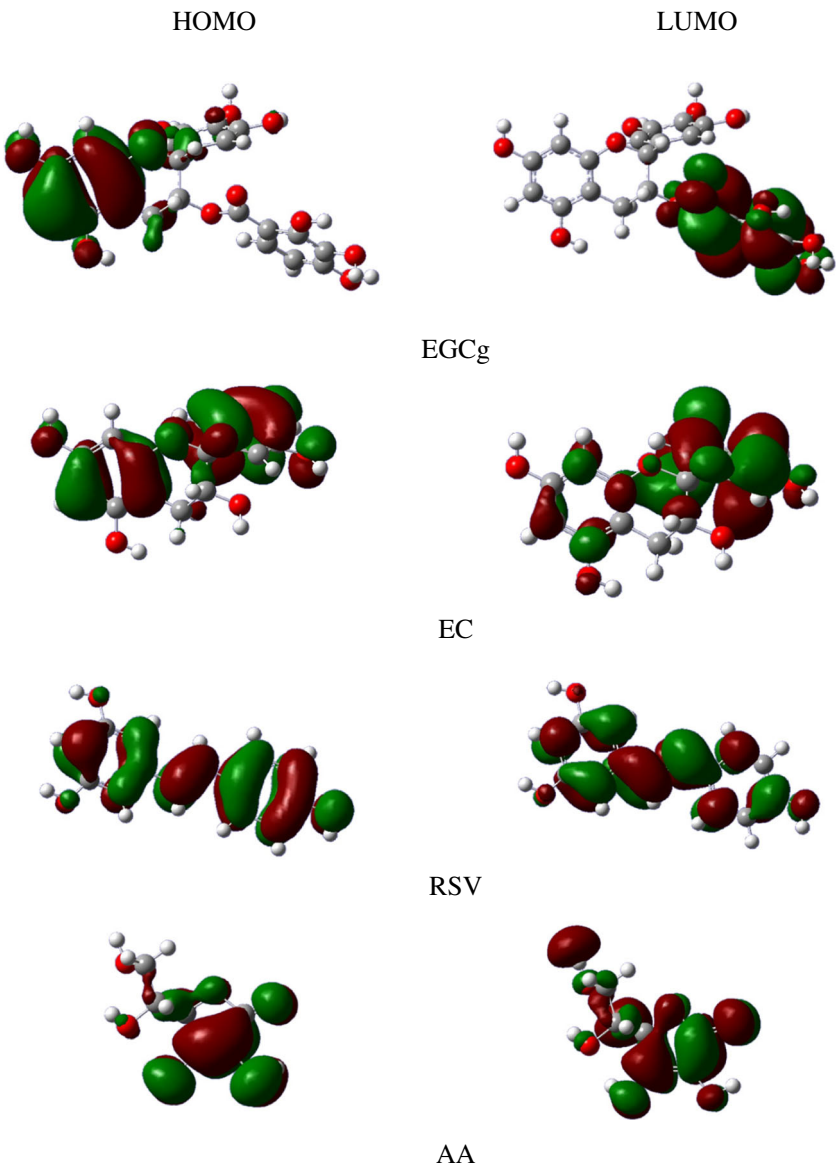

Fig. 4 HOMO and LUMO frontier orbitals of EGCg, EC, RSV, and AA

For AA, the unpaired electron in 2–O and 3–O radicals is mainly located on the pentacycle, while in the 5–O radical, unpaired electron is almost delocated over the whole radical. However, the spin density in 6–O radical is concentrated outside the pentacycle.

Electrostatic potential (ESP) is another important parameter, which is fundamental for understanding the chemical reactivity and the atomic structure of molecules [64]. In the ESP mapped surface, the negative potential energy (nucleophilic region) is colored in red and positive potential energy (electrophilic region) is colored in blue.

Figure 6 illustrates the ESP maps of studied compounds. Regarding EGCg, the gallate part of the molecule is electrophilic, and all OH groups are nucleophilic. For EC, the A ring and the 4′–OH site can accept an electrophilic attack.

If we consider the ESP map of RSV, we can see the dominance of the nucleophilic region with a small electrophilic character.

The ESP map of AA shows a predominance of the electrophilic region. The OH groups of the pentacycle have a nucleophilic character.

Overall, the results of the ESP show a concordance with the results of frontier orbitals (HOMO and LUMO).

Determination of acidity

To determine the acidity of polyphenols, two methods were investigated: (i) calculation of pKa and (ii) determination of the enthalpy difference between the anion (A^-) and its neutral species (HA).

Table 5 Mulliken spin densities on oxygen atom in radicals of EGCg, EC, RSV, and AA obtained by UHF/6-31G, B3LYP/6-311G(d,p), and B3LYP/6-311++G(d,p)

Radical	Method		
	UHF/6-31G	DFT B3LYP/6-311G(d,p)	DFT B3LYP/6-311++G(d,p)
EGCg-5–O	0.21	0.38	0.37
EGCg-7–O	0.20	0.48	0.47
EGCg-3′–O	0.19	0.42	0.41
EGCg-4′–O	0.23	0.39	0.38
EGCg-5′–O	0.19	0.36	0.35
EGCg-3″–O	0.18	0.39	0.39
EGCg-4″–O	0.24	0.41	0.40
EGCg-5″–O	0.19	0.41	0.40
EC-3–O	0.10	0.72	0.70
EC-5–O	0.19	0.38	0.37
EC-7–O	0.17	0.41	0.40
EC-5′–O	0.18	0.35	0.34
EC-4′–O	0.19	0.34	0.34
RSV-3–O	0.18	0.39	0.38
RSV-5–O	0.19	0.40	0.39
RSV-4′–O	0.13	0.31	0.30
AA-2–O	0.23	0.39	0.40
AA-3–O	0.15	0.26	0.26
AA-5–O	0.03	0.70	0.68
AA-6–O	0.01	0.85	0.84

As shown in Table 6, for our phenolic compounds (EGCg, EC, and RSV), the pKa values of the OH sites belonging to the A ring are between 10.04 and 11.46. Regarding the B ring, the pKas of the OH sites are 8.45 for 5′–OH of EC and 8.24 for 4′–OH of EC and RSV.

The pKa values in A and B rings are consistent with the PDE values which were found to be lower in the B ring than those in the A ring, for all three phenolic compounds.

The pKa values of the OH groups in the gallate moiety are the lowest. All pKa values for EGCg in the B ring are lower than 7.00, indicating that all OH sites of EGCg are more acidic than those of EC and RSV in the B ring.

It can be concluded that the high antioxidant activity of EGCg is in part related to the strong acidity of the OH groups, especially in the gallate moiety.

One of the antioxidant mechanisms of polyphenols is chelation of metals. Metals are entrapped in these polyphenols–metals complexes and are hence prevented from being involved in some reactions, such as the production of free radicals. Chelation of metals often occurs through deprotonated hydroxyls in the polyphenols.

The determination of the acidity of these compounds is an important thermodynamic parameter that must be taken into account. The smaller the energy required to deprotonate the OH groups (acidity), the easier the metals chelation will be.

On the basis of B3LYP/6-311++G(d,p) increasing acidity values, an order can be given by comparing the smallest enthalpy value of each molecule:

$$\text{EGCg}\ (1315.99\ \text{kJ/mol}) < \text{AA}\ (1349.31\ \text{kJ/mol}) < \text{EC}\ (1424.34\ \text{kJ/mol}) < \text{RSV}\ (1427.29\ \text{kJ/mol}).$$

Calculated acidity values are in the same trend of pKa values:

$$\text{For EGCg}: 5''\text{–OH} < 3''\text{–OH} < 4''\text{–OH} < 4'\text{–OH} < 3'\text{–OH} < 5'\text{–OH} < 5\text{–OH} < 7\text{–OH}.$$

$$\text{For EC}: 4'\text{–OH} < 5'\text{–OH} < 5\text{–OH} < 7\text{–OH} < 3\text{–OH}.$$

$$\text{For RSV}: 4'\text{–OH} < 3\text{–OH} < 5\text{–OH}.$$

The value of acidity for EGCg is the smallest (1315.99 kJ/mol). This finding is in agreement with all calculated parameters.

Conclusion

In this work, the antioxidant activities of flavonoids, epigallocatechin gallate (EGCg), and epicatechin (EC) were

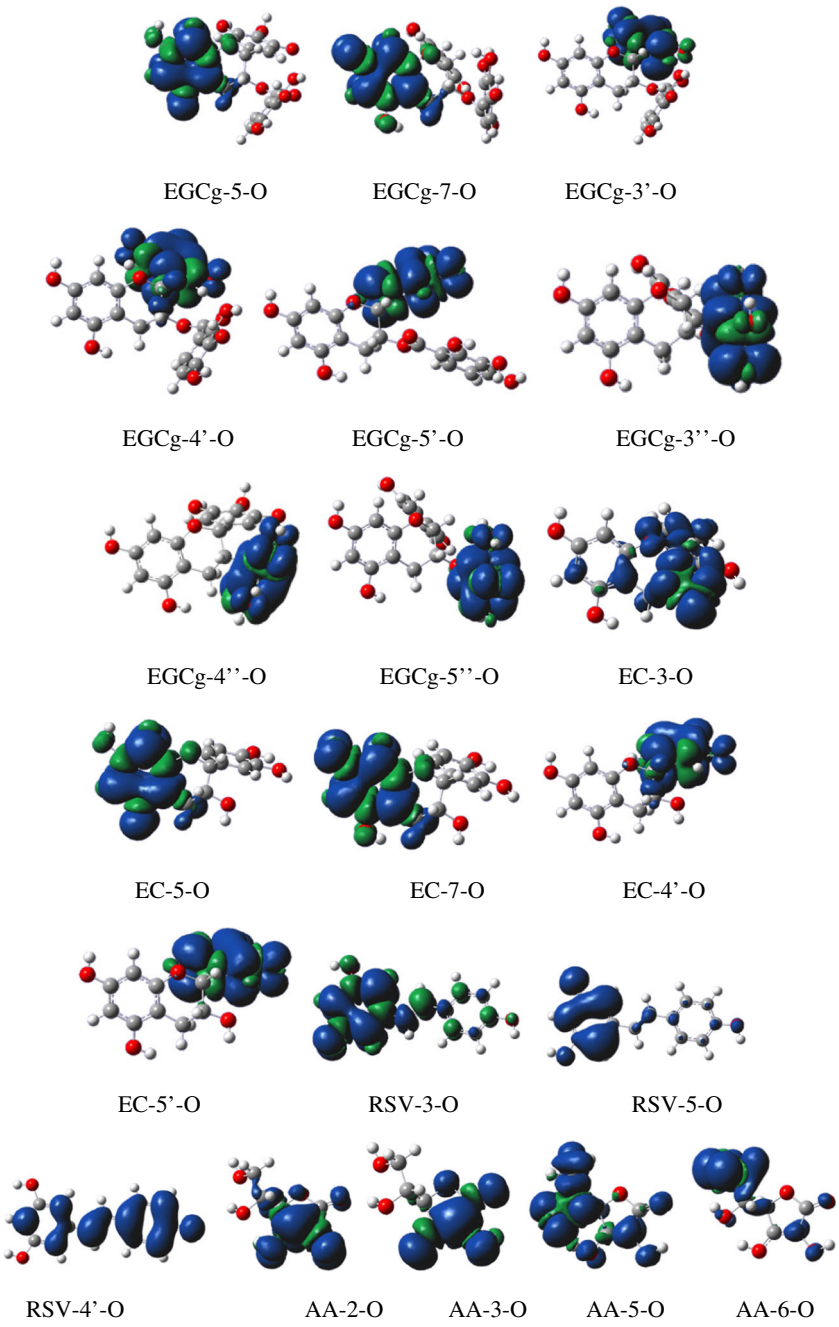

Fig. 5 Spin density images of EGCg, EC, RSV, and AA

determined by experimental and theoretical methods and compared to that of a stilbene, resveratrol (RSV), and ascorbic acid (AA) as a reference.

Results of the study of antioxidant activity, according to the iron reduction method, show that EGCg has a very interesting power to reduce the Fe^{3+} ion especially at very low concentrations. The DPPH free radical scavenging assay showed that the EGCg has an anti-radical activity greater than RSV but less than AA. Using DFT calculations in the gas phase, enthalpy values (BDE, AIP, PDE, PA, ETE, and acidity) and pKas of EGCg revealed that the gallate moiety and 4′–OH in the B ring are the most favored sites and are responsible for the higher antioxidant potential of these molecules compared to RSV.

For EC, the two sites 5′–OH and 4′–OH in the B ring are the most preferential active sites for the three mechanisms (HAT, SET-PT, and SPLET) and show an antioxidant capacity lower than EGCg but greater than RSV.

The three mechanisms of antioxidant activity (HAT, SET-PT, and SPLET) investigated are favored for EGCg. SET-PT is the most preferred antioxidant mechanism for the two

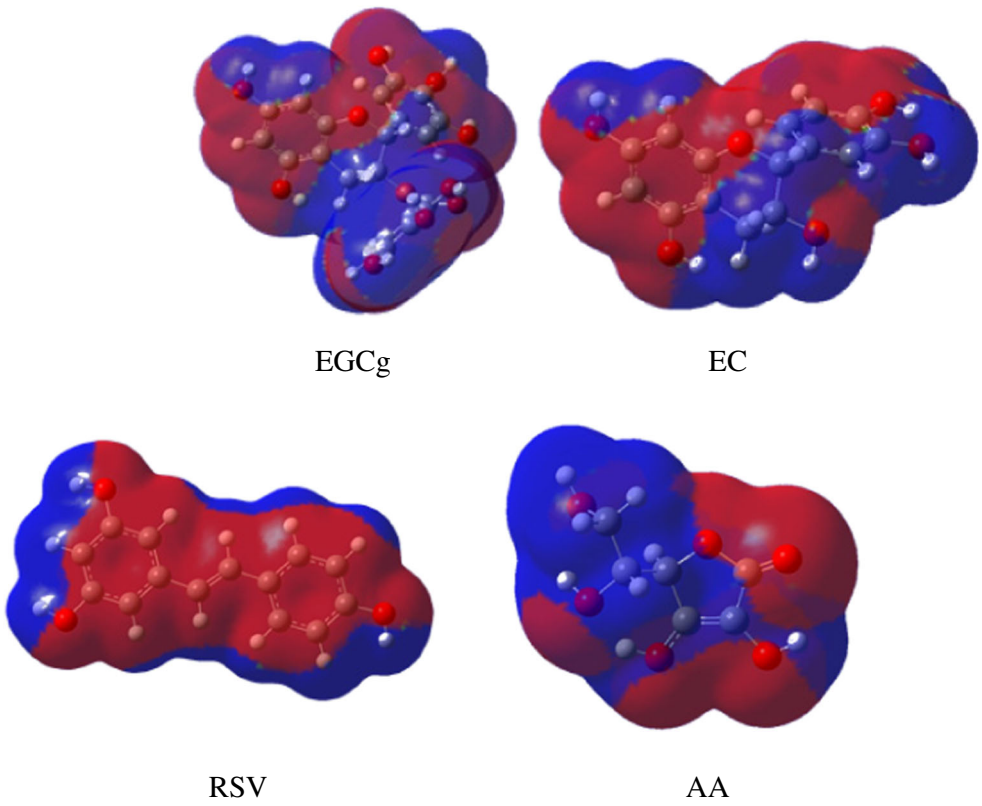

Fig. 6 Molecular electrostatic potential mapped on the isodensity surface of EGCg, EC, RSV, and AA at B3LYP/6-311++G(d,p) level of theory in gaseous phase

Table 6 Enthalpy of acidity in kJ/mol and pKa values for OH groups in EGCg, EC, RSV, and AA

Molecule		$\Delta H_{acidity}$	pka	Ring
EGCg	5–OH	1438.28	10.04	A
	7–OH	1456.87	11.44	A
	3′–OH	1403.32	6.70	B
	4′OH	1381.10	4.21	B
	5′–OH	1404.17	6.64	B
	3″–OH	1331.26	1.81	D
	4″–OH	1352.44	3.07	D
	5″–OH	1315.99	−0.65	D
EC	3–OH	1488.56	21.18	C
	5–OH	1439.24	10.30	A
	7–OH	1465.46	11.46	A
	5′–OH	1427.53	8.45	B
	4′–OH	1424.34	8.24	B
RSV	3–OH	1451.34	11.21	A
	5–OH	1453.78	11.44	A
	4′–OH	1427.29	8.24	B
AA	2–OH	1467.87	9.45	Inside the pentacycle
	3–OH	1364.75	0.26	Inside the pentacycle
	5–OH	1364.75	0.26	Ouside the pentacycle
	6–OH	1349.31	−0.98	Outside the pentacycle

catechins and it is the most suitable in the first step for resveratrol. The SPLET mechanism is favored for EC but to a lesser degree compared to EGCg.

Our results also show that there is a strong relation between BDE and spin density for EC and RSV since these two parameters follow the same trend for all radicals.

In water, the second step of SET-PT and the first step of SPLET are the most thermodynamically favored mechanisms compared to HAT mechanism for the studied molecules.

Evaluation of acidity of hydroxyl groups by determining both pKa and enthalpy difference between the anion (A^-) and neutral species (HA) showed that higher antioxidant activity of EGCg is in part related to strong acidity of its OH groups; indeed, all OH sites of EGCg, especially in the gallate moiety, are more acidic than those of EC and RSV. Results of pKa of studied molecules reinforce the other computed thermodynamic parameters.

The reactivity of molecules was evaluated by mapping ESP surfaces which showed that resveratrol presents a nucleophilic character, while EGCg and EC are rather electrophilic but possess some nucleophilic regions which indicates that studied molecules are good proton donors.

It should be stressed that Mulliken spin density for radicals obtained by DFT method agree better with the other calculated parameters than those obtained by HF method.

Moreover, the use of diffuse function has almost no impact on the spin density values; however, it caused a decrease in HOMO and LUMO energies.

Regarding the concordance of experimental and theoretical results, there is a good correlation between DPPH scavenging assay and calculated thermodynamic and electronic parameters.

Finally, we can conclude that the two flavonoids EGCg and EC are more potent antioxidants than the stilbene RSV.

This study could be extended to peruse the effect of different attracting and withdrawing substituents on this trend.

Author contribution Y. Boulmokh: investigation, methodology, writing, original draft, review, and editing.

K. Belguidoum: investigation, original draft of the experimental part, and review.

F. Meddour: contribution in the theoretical part.

H. Amira-Guebailia: supervision, investigation, methodology, original draft, writing, and review.

Declarations

Consent to publish

All authors whose names appear on the submission approved the version to be published.

Conflict of interest The authors declare that they have no competing interests.

References

1. Rahardiyan D (2019). Food Res 3:1–6
2. Vestergaard M, Ingmer H (2019). Int J Antimicrob Agents 53:716–723
3. Jamróz E, Kulawik P, Krzyściak P, Talaga-Ćwiertnia K, Juszczak L (2019). Int J Biol Macromol 122:745–757
4. Paulo L, Ferreira S, Gallardo E, Queiroz JA, Domingues F (2010). World J Microbiol Biotechnol 26:1533–1538
5. Nagaoka S, Nakayama N, Teramae H, Nagashima U (2019). Chem. Phys 522:77–83
6. Liu B, Yan W (2019). Food Chem 272:663–669
7. Iuga C, Alvarez-Idaboy JR, Russo N (2012). J Org Chem 77:3868–3877
8. Ke F, Zhang M, Qin N, Zhao G, Chu J, Wan X (2019). J Mater Sci 54:10420–10429
9. Gianchecchi E, Fierabracci A (2020). Antioxidants 9:91–107
10. Natarajan SB, Chandran SP, Vinukonda A, Rajan S (2019). Asian J Pharm Clin Res 12:1–7
11. Farzaei M H, Bahramsoltani R, Abbasabadi Z, Braidy N, Nabavi S M (2018) J Cell Physiol 1–13
12. Pervin M, Unno K, Takagaki A, Isemura M (2019). Int J Mol Sci 20:3630
13. Pérez-González A, Rebollar-Zepeda AM, León-Carmona JR, Galano A (2012). J Mex Chem Soc 56:241–249
14. Rice-Evans CA, Miller NJ, Paganga G (1996). Free Radical Biol Med 20:933–956
15. Bendary E, Francis RR, Ali HMG, Sarwat MI, El Hady S (2013). Ann Agric Sci 58:173–181
16. Anouar E, Raweh S, Bayach I, Taha M, Baharudin MS, Meo FD, Hasan MH, Adam A, Ismail NH, Weber JF, Trouillas P (2013). J Comput Aided Mol Des 27:951–964
17. Kongpichitchoke T, Hsu J, Huang T (2015). J Agric Food Chem 63:4580–4586
18. Shahidi F, Ambigaipalan P (2015). J Funct Foods 18:820–897
19. Uranga JG, Podio NS, Wunderlin DA, SantiagoA N (2016). ChemistrySelect 1:4113–4120
20. Caoa H, Chenga W, Lia C, Pana X, Xiea X, Lia T (2005). J Mol Struct 719:177–183
21. Sadasivam K, Kumaresan R (2011). Mol Phys 109:839–852
22. Sarkar A, Middya TR, Jana AD (2012). J Mol Model 18:2621–2631
23. Anouar E, Ali Shah SA, Hassan NB, El Moussaoui N, Ahmad R, Zulkefeli F, Weber JF (2014). Molecules 19:3489–3507
24. Muglu H, Çavus MS¸ Bakır T, Yakan H (2019) J Mol Struct 1196: 819-827.
25. Mohajeri A, Asemani SS (2009). J Mol Struct 930:15–20
26. Wang J, Tang H, Hou B, Zhang P, Wang Q, Zhang B, Huang Y, Wang Y, Xiang Z, Zi C, Wang X, Sheng J (2017). RSC Adv 7: 54136–54141
27. Bougandoura N, Bendimerad N (2013) NATEC 14–19
28. Ferreira ICFR, Aires E, Barreira JCM, Estevinho LM (2009). Food Chem 114:1438–1443
29. Anitha S, Krishnan S, Senthilkumar K, Sasirekha V (2020). Mol Phys:118
30. Josefredo R, Pliego J (2003). Chem Phys Lett 367:145–149
31. Kelly CP, Cramer CJ, Truhlar DG (2005). J Chem Theory Comput 1:1133–1152
32. Frisch MJ, Trucks GW, Schlegel HB, Scuseria GE, Robb MA, Cheeseman JR, Scalmani G, Barone V, Mennucci B, Petersson GA, Nakatsuji H, Caricato M, Li X, Hratchian HP, Izmaylov AF, Bloino J, Zheng G, Sonnenberg JL, Hada M, Ehara M, Toyota K, Fukuda R, Hasegawa J, Ishida M, Nakajima T, Honda Y, Kitao O, Nakai H, Vreven T, Montgomery Jr JA, Peralta JE, Ogliaro F, Bearpark M, Heyd JJ, Brothers E, Kudin KN, Staroverov VN, Kobayashi R, Normand J, Raghavachari K, Rendell A, Burant JC, Iyengar SS, Tomasi J, Cossi M, Rega N, Millam JM, Klene M, Knox JE, Cross JB, Bakken V, Adamo C, Jaramillo J, Gomperts R, Stratmann RE, Yazyev O, Austin AJ, Cammi R, Pomelli JW, Ochterski C, Martin RL, Morokuma K, Zakrzewski VG, Voth GA, Salvador P, Dannenberg JJ, Dapprich S, Daniels AD, Farkas O, Foresman JB, Ortiz JV, Cioslowski J, Fox DJ (2009) GAUSSIAN 09 A. Program package Gaussian Inc., Wallingford
33. He J, Xu L, Yang L, Wang X (2018). Med Sci Monit. 24:8198–8206
34. Guo Q, Zhao B, Shen S, Hou J, Hu J, Xin W (1999). Biochim Biophys Acta 1427:13–23
35. Nanjo F, Goto K, Seto R, Suzuki M, Sakai M, Hara Y (1996). Free Radical Biol Med 21:895–902
36. Zaiter A, Becker L, Karam M, Dicko A (2016). J Food Sci Technol 53:2025–2032
37. Grzesik M, Naparło K, Bartosz G, Sadowska-Bartosz I (2018). Food Chem 241:480–492
38. Lu L, Zhu S, Zhang H, Zhang S (2013). Comput Theor Chem 1019: 39–47
39. Nazarparvar E, Zahedi M, Klein E (2012). J Org Chem 77:10093–10104
40. Thi TP, The SN (2020). J Chem 2020:1–15
41. Jabeen H, Saleemia S, Razzaq H, Yaqub A, Shakoor S, Qureshi R (2018). J Photochem Photobiol B Biol 180:268–275
42. Albuquerque VR, Malcher SN, Amado LL, Coleman DM, dos Santos CD, Sa Borges R, Valente SSA, Valente CV, Monteiro MC (2015). PLOS One 10:e0134768
43. Leopoldini M, Russo N, Toscano M (2011). Food Chem 125:288–306
44. Mikulski D, Górniak R, Molski M (2010). Eur J Med Chem 45: 1015–1027

45. Mikulski D, Szelag M, Molski M, Górniak R (2010). Theor Chem 951:37–48
46. Benayahoum A, Amira-Guebailia H, Houache O (2014). Comput Theor Chem 1037:1–9
47. Mikulski D, Molski M (2010). Eur J Med Chem 45:2366–2380
48. Fukuhara K, Nakanishi I, Matsuoka A, Matsumura T, Honda S, Hayashi M, Ozawa T, Miyata N, Saito S, Ikota N, Okuda H (2008). Chem Res Toxicol 21:282–287
49. Vagánek A, Rimarčík J, Lukeš V, Klein E (2006). Biochim Biophys Acta 1757:969–980
50. Zheng Y, Chen D, Deng G, Guo R, Fu Z (2018). Phytochemistry 156:184–192
51. Lengryel J, Rimarčík J, Vagánek A, Klein E (2013). Phys Chem Chem Phys 15:10895–10903
52. Xue Y, Zheng Y, An L, Dou Y, Liu Y (2014). Food Chem 151: 198–206
53. Sadasivam K, Kumarisan R (2011). Comput Theor Chem 963:227–235
54. Queiroz AN, Gomes BAQ, Moraes Jr WM, Borges RS (2009). Eur J Med Chem 44:1644–1649
55. Zhou C, Deng F, Li T (2003) Bioorg Cao H, Pan X, Li C Med Chem Lett 13: 1869-1871
56. Benayahoum A, Amira-Guebailia H, Houache O (2013). J Mol Model 19:2285–2298
57. Liu L, Li Y, Oguzie E, Wang F (2015). J Ind Eng Chem 26:18 Chidiebere 2-192
58. Lewars EG (2003) Kluwer Academic Publishers Norwell
59. Hatch FT, Lightstone FC, Colvein ME (2000). Environ Mol Mutagen 35:279–299
60. Akhtari K, Hassanzadeh K, Fakhraei B, Fakhraei N, Hassanzadeh H, Akhtari G, Zarei SA, Hassanzadeh K (2015). Monatsh Chem 146:601–611
61. Filatov M, Cremer D (2005). J Chem Phys 123:124101–124107
62. Giner E, Angeli C (2016). J Chem Phys 144:104104-1–104104-12
63. Macetti G, Presti LL, Gatti C (2018). J Comput Chem 39:587–603
64. Hubschle CB, Smaalen SV (2017). J Appl Cryst 50:1627–1636